UV Resonance Raman Studies of α-Nitrosyl Hemoglobin Derivatives: Relation between the α1−β2 Subunit Interface Interactions and the Fe−Histidine Bonding of α Heme†

S. Nagatomo,‡ M. Nagai,§ A. Tsuneshige,|| T. Yonetani,|| and T. Kitagawa*,‡

Institute for Molecular Science, Okazaki National Research Institutes, Myodaiji, Okazaki, 444-8585, Japan, School of Health Sciences, Faculty of Medicine, Kanazawa University, Kanazawa 920-0942, Japan, and Department of Biochemistry & Biophysics, School of Medicine, University of Pennsylvania, Philadelphia, Pennsylvania 19194-6089

Received March 11, 1999; Revised Manuscript Received May 17, 1999

ABSTRACT: Human α-nitrosyl β-deoxy hemoglobin A, $\alpha^{NO}\beta^{deoxy}$, is considered to have a T (tense) structure with the low O_2 affinity extreme and the Fe−histidine (His87) (Fe−His) bond of α heme cleaved. The Fe−His bonding of α heme and the intersubunit interactions at the α1−β2 contact of α^{NO}-Hbs have been examined under various conditions with EPR and UV resonance Raman (UVRR) spectra excited at 235 nm, respectively. NOHb at pH 6.7 gave the UVRR spectrum of the R structure, but in the presence of inositol-hexakis-phosphate (IHP) for which the Fe−His bond of the α heme is broken, UVRR bands of Trp residues behaved half-T-like while Tyr bands remained R-like. The half-ligated nitrosylHb, $\alpha^{NO}\beta^{deoxy}$, in the presence of IHP at pH 5.6, gave T-like UVRR spectra for both Tyr and Trp, but binding of CO to its β heme ($\alpha^{NO}\beta^{CO}$) changed the UVRR spectrum to half-T-like. Binding of NO to its β heme (NOHb) changed the UVRR spectrum to 70% T-type for Trp but almost R-type for Tyr. When the pH was raised to 8.2 in the presence of IHP, the UVRR spectrum of NOHb was the same as that of COHb. EPR spectra of these Hbs indicated that the Fe−His bond of α^{NO} heme is partially cleaved. On the other hand, the UVRR spectra of $\alpha^{NO}\beta^{deoxy}$ in the absence of IHP at pH 8.8 showed the T-like UVRR spectrum, but the EPR spectrum indicated that 40−50% of the Fe−His bond of α hemes was intact. Therefore, it became evident that there is a qualitative correlation between the cleavage of the Fe−His bond of α heme and T-like contact of Trp-β37. We note that the behaviors of Tyr and Trp residues at the α1−β2 interface are not synchronous. It is likely that the behaviors of Tyr residues are controlled by the ligation of β heme through His-β92(F8)→Val-β98(FG5)→Asp-β99(G1)→Tyr-α42(C7) or Tyr-β145(HC2).

Human hemoglobin A (Hb)[1] with the $\alpha_2\beta_2$ tetramer structure, exhibiting positive cooperativity in oxygen binding, has been extensively investigated, since it serves as a model of general allosteric proteins (*1*) and, currently, elucidation of a structural mechanism of cooperativity is a major subject of Hb studies. X-ray crystallographic studies have demonstrated the presence of two distinct quaternary structures, called T (tense) and R (relaxed) structures, which correspond to the low-affinity and high-affinity states, respectively, and whose typical structures are seen for the deoxy and CO-bound forms, respectively (*2*). The cooperative oxygen binding of Hb has been explained in terms of a reversible transition between the two quaternary structures upon partial ligation of four hemes (*3, 4*). The largest structural differences between the T and R structures, revealed by X-ray crystallographic analysis (*5*), are located in the α1−β2 subunit interface, where resets of hydrogen bonds and salt-bridges take place upon ligation to deoxyHb. The ^{1}H NMR signal of Tyr-α42,which forms a hydrogen bond with Asp-β99 in the T state but is free in the R state, has served as a diagnostic marker for the quaternary structure (*6, 7*).

Nitric oxide (NO), which binds to deoxyHb similar to CO and O_2 but with much higher affinity (>1000 times) than CO and O_2 (*8*) and forms an NO adduct (NOHb), is an unusual ligand. Addition of an effector, inositol-hexakis-phosphate (IHP), to NOHb changes its UV absorption and CD spectra, sulfhydryl reactivities, and exchangeable ^{1}H NMR signals sensitive to the R → T transition, although carbonmonoxyHb (COHb) and oxyHb exhibit no such changes. NO binds preferentially to the α subunit (affinity is 10 times higher to the α subunit than to the β subunit) in the presence of IHP (*9*), causing the transformation of Hb to a low-affinity extreme. Since there is no Bohr effect and no cooperativity in this state, it is conveniently called the 'T-(low affinity extreme)' state in this paper, which has been explicitly defined in ref *10*. Indeed, NO has been successfully applied as clinical treatment of newborns with persistent

† This study was supported by Grants-in-Aid for Scientific Research on Priority Areas (Molecular Biometallics) from the Ministry of Education, Science, Sports, and Culture, Japan, to T.K. (08249106) and M.N. (11116209) and by U.S. National Heart, Lung, and Blood Institute Grant HL14508 to T.Y.

* To whom correspondence should be addressed.
‡ Okazaki National Research Institutes.
§ Kanazawa University.
|| University of Pennsylvania.

[1] Abbreviations: Hb, hemoglobin A; NOHb, nitrosylHb; COHb, carbonmonoxyHb; IHP, inositol-hexakis-phosphate; RR, resonance Raman; UVRR, ultraviolet resonance Raman; $\alpha^{NO}\beta^{deoxy}$, α-nitrosyl β-deoxyHb; $\alpha^{NO}\beta^{CO}$, α-nitrosyl β-carbonmonoxyHb; $\alpha^{Fe}\beta^{Ni}$, α(Fe)β-(Ni) metal hybrid Hb.

10.1021/bi990567w CCC: $18.00
Published on Web 07/03/1999

pulmonary hypertension with no apparent acute adverse effect. The half-ligated α-nitrosyl β-deoxy hemoglobin, $\alpha^{NO}\beta^{deoxy}$, is stable and binds O_2 without cooperativity. When O_2 is bound to the β subunit of $\alpha^{NO}\beta^{deoxy}$, EPR study indicated its conversion to the high-affinity state under ordinary conditions but it remained in the low-affinity state in the presence of IHP at pH 4.8 (*10*).

NOHb normally contains the six-coordinate hemes, but, in the presence of IHP, the visible absorption (*11*), EPR (*12*−*14*), and resonance Raman studies (*15*) indicated cleavage of the Fe−His bond of α-NO hemes (α^{NO}) with no change for the β-NO hemes (β^{NO}). This change of the α^{NO} heme seems to generate the T-(low affinity extreme) state in the β^{deoxy} hemes. It is known that the Fe−His bond strength, reflected by the Fe−His stretching frequency, sensitively reflects the quaternary structure of Hb (*16*) and the Fe−His bond strength is weaker in the α than β subunit in the T state while they are similar in the R state (*17*). These facts may suggest that the intersubunit interactions at the $\alpha1-\beta2$ interface have close correlation with the Fe−His bonding of the α subunit, while details remain to be clarified.

It has been demonstrated recently that resonance Raman (RR) spectra excited in the UV region around 220−240 nm can explore the environmental and hydrogen-bonding changes of Trp and Tyr residues of proteins (see refs *18* and *19* for a review). In fact, Rodgers et al. (*20*, *21*), Nagai, M., et al. (*22*, *23*), Huang et al. (*24*, *25*), Hu et al. (*26*, *27*), and Peterson and Friedman (*28*) reported the quaternary structure dependent features for Tyr and Trp residues in the $\alpha1-\beta2$ interface of Hb from 230- and 235-nm excited UVRR spectra. In this paper, we present 235-nm excited UVRR spectra for normal NOHb, the half-ligated $\alpha^{NO}\beta^{deoxy}$, and the mix-ligated $\alpha^{NO}\beta^{CO}$ in the presence and absence of IHP at several pH values, discussing possible correlation between the Fe−His bonding of α hemes and intersubunit interactions at the $\alpha1-\beta2$ interface for the quaternary structure change.

EXPERIMENTAL PROCEDURES

Hemoglobin A was purified from fresh human blood by a preparative isoelectric focusing electrophoresis (*29*). Approximately 150 μL of the Hb solution (400 μM in heme) was put into a spinning cell made of a synthetic quartz ESR tube (diameter = 5 mm) (*30*). DeoxyHb and COHb were prepared by adding sodium dithionite (1 mg/mL) to oxyHb after replacement of the inside air of the sample tube with N_2 and CO, respectively. NOHb was obtained by addition of NO, which had been in advance passed through 1 M NaOH solution, to deoxyHb. The NO/O_2-mixed-ligated Hb, $\alpha^{NO}\beta^{O2}$, was prepared by mixing equal amounts of isolated α-NO and β-O_2 chains, while a method for the preparation of the isolated α-NO chain was described elsewhere (*10*). The half-ligated Hb, $\alpha^{NO}\beta^{deoxy}$, was obtained through addition of a small amount of sodium dithionite to $\alpha^{NO}\beta^{O2}$. The NO/CO-mixed-ligated Hb, $\alpha^{NO}\beta^{CO}$, was prepared by adding CO to $\alpha^{NO}\beta^{deoxy}$.

Just before the measurements of UVRR spectra, Na_2SO_4 was added to samples at a final concentration of 0.2 M as an internal intensity standard of Raman spectra. It was confirmed that the addition of sulfate did not cause any apparent Raman spectral change for the states examined in this study, since its use in UVRR experiments was warned against due to possible tertiary structure change (*31*). IHP was added to samples at a final concentration of 5 mM just before the Raman measurement. We used sodium acetate buffer under pH 6, phosphate buffer for the pH region from pH 6.5 to 7.5, and Tris buffer or borate buffer over pH 8.

UVRR spectra were excited by a XeCl excimer laser-pumped dye laser system (EMG103MSC/LPX120 and FL2002/SCANMATE, Lambda Physik). The 308-nm line from a XeCl excimer laser (operated at 100 Hz) was used to excite coumarin 480, and the 470-nm output from the dye laser was frequency-doubled with a β-BaB_2O_4 crystal to generate 235-nm pulses. The Raman excitation light (15 μJ/pulse) was illuminated to the area of 0.2×3 mm^2 of sample cell from the lower front side. The scattered light was dispersed with an asymmetric double monochromator (Spex 1404) in which the gratings in the first and second dispersion steps are 2400 grooves/mm (holographic) and 1200 grooves/mm (machine-ruled, 500-nm blaze), respectively, and detected by an intensified photodiode array (PC-IMD/C5222-0110G) (*32*).

The spinning cell was moved vertically by 1 mm for every spectrum (every 5 min) to shift the laser illumination spot on the sample (*30*). The temperature of the sample solution was kept at 10 °C by flushing with cooled N_2 gas against the cell. The scattered light was collected with Cassegrainian optics with f/1.1. One spectrum is composed of the sum of 400 exposures, each exposure accumulating the data for 0.8 s. The Raman spectra shown in the figures are averages of 8−25 spectra. Raman shifts were calibrated with cyclohexane. Denaturation of the samples due to exposure to the ultraviolet laser light was carefully checked by inspecting a possible change in the visible absorption spectrum before and after the measurements of UVRR spectra. If some spectral changes were recognized, the Raman spectrum was discarded. Visible absorption measurements were carried out with a Hitachi 220S spectrophotometer.

EPR spectra were measured with a Varian X-band EPR spectrometer, Model E109 (Varian Associates, CA), integrated with a data acquisition system (Scientific Software Services, IL). EPR samples (300 μL of 500 μM heme) in quartz EPR tubes (3-mm precision bore) were frozen by immersion into liquid nitrogen and measured at liquid nitrogen temperature. The spectrometer was operated at a microwave frequency of 9.11GHz, microwave power of 20 mW, modulation frequency of 100 kHz, modulation amplitude of 2.0 G, magnetic field scan rate of 125 G/min, and time contant of 0.2 s. Recorded EPR data were manipulated with EPR software (Scientific Software Services) for quantitative analyses.

RESULTS

Figure 1 shows the 235-nm excited UVRR spectra for deoxyHb (A), COHb (B), and their difference (C = A − B) at pH 6.7 in the frequency region from 1700 to 700 cm^{-1}. Although a strong broad band due to a synthetic quartz cell appeared between 800 and 900 cm^{-1}, its contribution was subtracted from the spectra shown here. The band at 982 cm^{-1} arises from SO_4^{2-} ions and was used to normalize the intensity of the spectra (*33*). In the spectrum of deoxyHb, RR bands of Tyr are seen at 1619 (Y8a), 1208 (Y7a), 1178 (Y9a), and 854 cm^{-1} (Y1), and those of Trp are seen at 1558

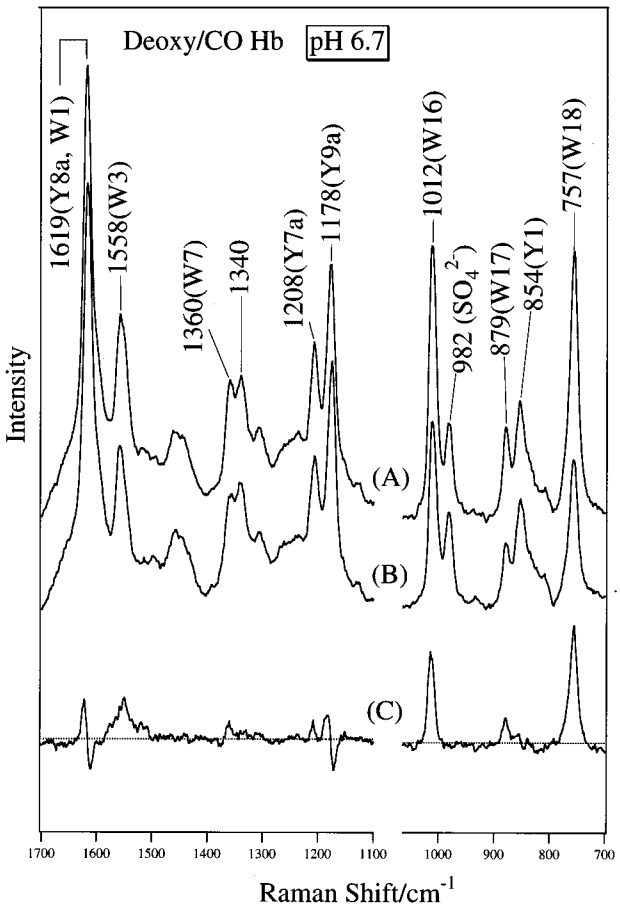

FIGURE 1: 235-nm excited UVRR spectra of deoxyHb (A), COHb (B), and their difference spectra (C) (=deoxy Hb − COHb). Hb samples were equilibrated with 0.05 M phosphate buffer, pH 6.7, containing 0.2 M Na_2SO_4. Hb concentration was 400 μM in heme. Each spectrum is an average of 25 spectra. The ordinate scale of the difference spectrum is the same as those of raw spectra. All samples do not contain IHP. The band marked by SO_4^{2-} means the totally symmetric stretching band of SO_4^{2-} ions.

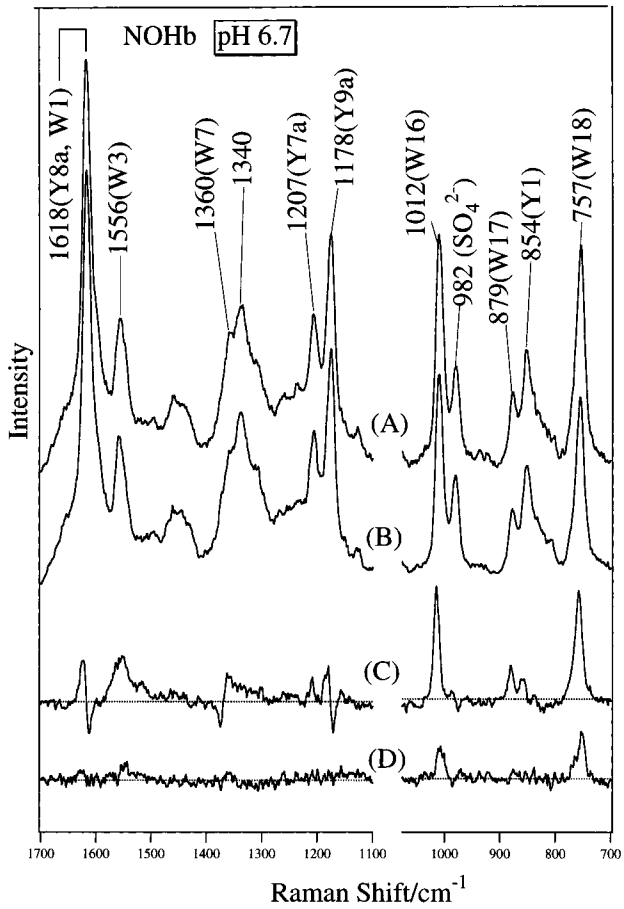

FIGURE 2: UVRR spectra of NOHb at pH 6.7 in the presence of IHP (A) and in its absence (B), the difference spectrum deoxyHb minus NOHb(−IHP) (C), and the difference spectrum NOHb-(+IHP) − NOHb(−IHP) (D). Sample conditions are the same as those in Figure. 1. The concentration of IHP was 5 mM. Each spectrum is an average of 10 spectra. The ordinate scales of the difference spectra are the same as those of raw spectra, and the spectrum of deoxyHb is the same as Figure 1(A). The band marked by SO_4^{2-} means the totally symmetric stretching band of SO_4^{2-} ions.

(W3), 1360−1340 (W7; tryptophan doublet), 1012 (W16), 879 (W17), and 757 cm^{-1} (W18). The assignments are based on Harada and co-workers (*18, 34, 35*). The UVRR spectra of deoxy Hb and COHb in the 1700−850 cm^{-1} region are in agreement with those reported by Rodgers et al. (*20*) and Nagai, M., et al. (*22*), while the spectra between 850 and 700 cm^{-1} are newly added. It was confirmed that the spectra of deoxyHb and COHb exhibited negligible changes upon addition of IHP (not shown).

The difference spectrum between deoxyHb and COHb (C) indicates that the intensities of the W3, W16, W17, and W18 bands of Trp are much weaker for COHb than for deoxyHb, while the peak positions remain unaltered, and that the frequencies of the Y8a and Y9a bands of Tyr are lower for COHb than for deoxyHb. These differences arise from some differences in hydrogen bonding states and surrounding hydrophobicity of Trp and Tyr residues between the two states (*36*) and have been ascribed to a consequence of changes in subunit contacts (*20*−*28, 37*). Hereafter spectrum (C) is referred to as the standard for the T minus R difference spectrum, reflecting the typical changes at the $\alpha1-\beta2$ subunit interface upon quaternary structure transition ("T-like" and "R-like" will be used to represent that the local structure surrounding a particular residue in question is similar to that in the ordinary T and R subunit contact, but it does not always mean that the tertiary structure is T and R, respectively).

Figure 2 shows the UVRR spectra of NOHb in the presence (A) and absence (B) of IHP at pH 6.7 and their difference (D) in addition to the difference (C) between deoxyHb and NOHb in the absence of IHP. A relatively strong band appeared around ∼1340 cm^{-1} in the raw spectrum of NOHb. This band is due to NO_2^- ions produced from NO in water. The UVRR spectrum of NO_2^- ions in water was measured separately and subtracted from the spectrum of NOHb prior to the difference calculations. As shown by spectrum (C), the difference spectrum between deoxyHb and NOHb is almost the same as spectrum Figure 1(C), suggesting that NOHb in the absence of IHP has an R-like $\alpha1-\beta2$ contact similar to COHb. Addition of IHP, however, causes distinct spectral changes especially on Trp bands; the intensities of the W3, W16, and W18 bands increased. The magnitude of the intensity increase of Trp bands is nearly half of those seen in the standard T minus R difference spectrum (Figure 1C), when the intensity of the SO_4^{2-} band is referred. It is noted that the peak positions of Tyr bands are not shifted upon addition of IHP. Therefore,

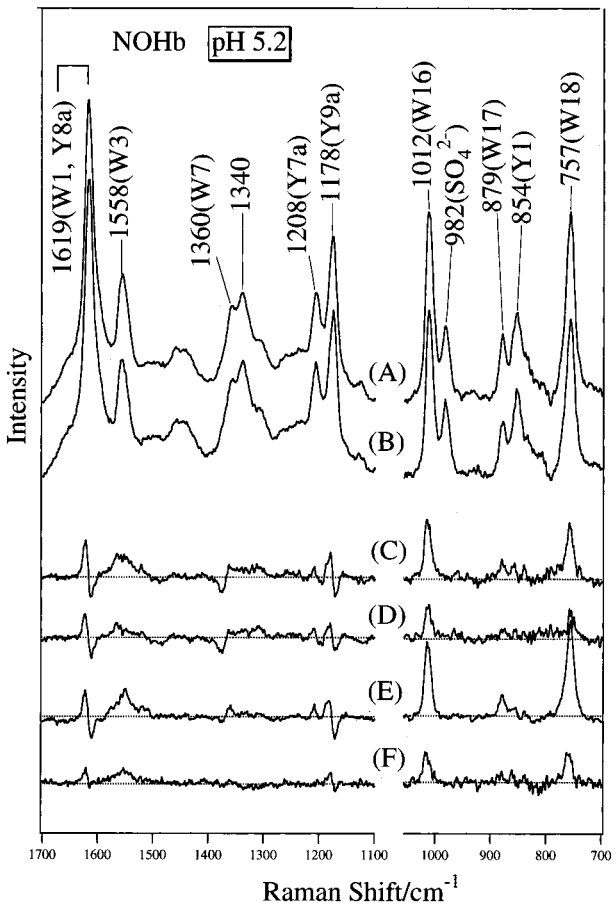

FIGURE 3: UVRR spectra of NOHb at pH 5.2 in the presence (A) and absence (B) of IHP, and difference spectra: (C) deoxyHb at pH 6.7 − (B); (D) deoxyHb at pH 6.7 − (A); (E) Figure 1(C); and (F) (A) − (B). The NOHb sample at pH 5.2 was equilibrated with 0.05 M acetate buffer. The concentration of IHP was 5 mM. The spectrum of deoxyHb is the same as Figure 1(A). Each spectrum is an average of 10 or 15 spectra. The band marked by SO_4^{2-} means the totally symmetric stretching band of SO_4^{2-} ions.

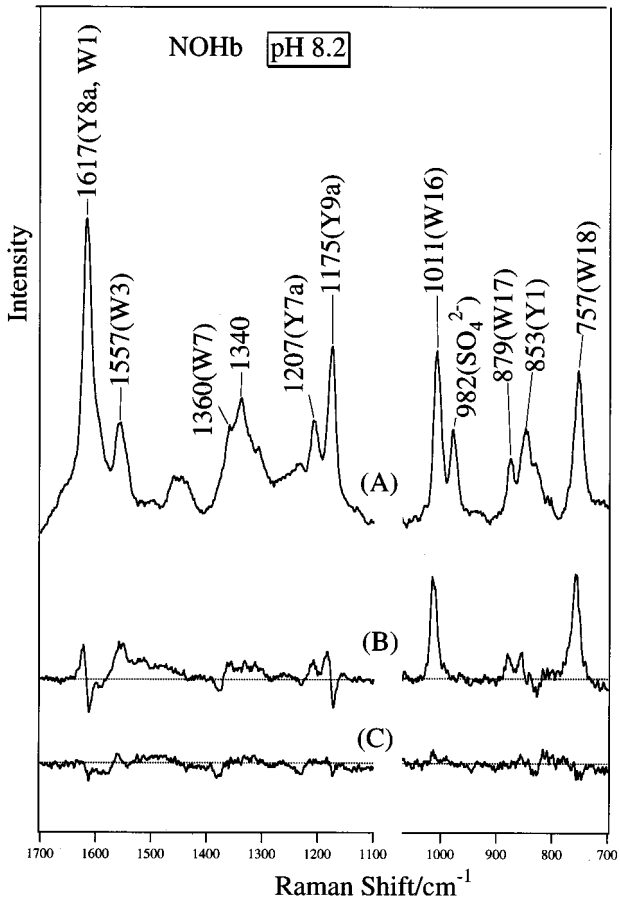

FIGURE 4: UVRR spectrum of NOHb at pH 8.2 in the presence of IHP (A) and difference spectra: (B) deoxyHb at pH 6.7 − (A); (C) COHb at pH 6.7 − (A). The NOHb sample at pH 8.2 was equilibrated with 0.05 M borate buffer. The concentration of IHP was 5 mM. Spectra of deoxyHb and COHb are the same as those in Figure 1. Each spectrum is an average of 10 spectra. The band marked by SO_4^{2-} means the totally symmetric stretching band of SO_4^{2-} ions.

Tyr residues of NOHb in the presence of IHP adopt the same structure as that in the R structure, while Trp residues are half-T-like structure (half may mean either the number of residues involved or all residues with half strength). Thus, the behaviors of Trp and Tyr residues are not always synchronous with the change of subunit contacts.

Figure 3 shows the UVRR spectra of NOHb in the presence (A) and absence (B) of IHP at pH 5.2 in the frequency region from 1700 to 700 cm^{-1}. There has been no difference between spectra of deoxyHb at pH 6.7 and 5.2. The difference spectra between deoxyHb and NOHb in the absence (C) and presence (D) of IHP at pH 5.2 are somewhat dissimilar to each other, and both are appreciably different from the standard T − R difference spectrum [reproduced by (E)]. In the absence of IHP, the difference spectrum (C) is apparently the same as that between deoxyHb and COHb (E), while detailed analysis has clarified the presence of an intensity difference in Trp bands, especially W16 and W18 [weaker in (C)]. This means that the structure of Trp in HbNO (−IHP) is somewhat different from that in COHb. The intensity patterns of Tyr in spectra (C) and (E) are alike. In the presence of IHP (D), the intensities of Trp bands are weaker, indicating that the structures of Trp residues become closer to those of deoxyHb, while Tyr bands are slightly affected by IHP. The difference spectrum of NOHb between the presence and absence of IHP (F) shows weak but definite changes for Tyr bands in addition to those of Trp bands. It is evident from the comparison of Figure 3(F) with Figure 2(D) that the effect of IHP was recognized only for Trp bands at pH 6.7 but for both Tyr and Trp bands at pH 5.2.

Figure 4 shows the UVRR spectrum of NOHb in the presence of IHP at pH 8.2. The spectrum remained unchanged between the presence and absence of IHP. Its difference spectra with regard to deoxyHb and COHb are depicted by spectra (B) and (C), respectively. Spectrum (B) is almost the same as Figure 1(C), and there are no clear difference peaks in spectrum (C), meaning that the subunit interface structures of NOHb in the presence of IHP at pH 8.2 resemble those of COHb, and effects of IHP as an allosteric effector are small.

Figure 5 shows the UVRR spectra of the half-ligated Hb, $\alpha^{NO}\beta^{deoxy}$, in the presence of IHP at pH 5.6 (A) and in its absence at pH 8.8 (B) in the frequency region from 1700 to 700 cm^{-1}. It was confirmed by EPR that there was no detectable migration of NO from the α^{NO} to the β^{deoxy} heme in $\alpha^{NO}\beta^{deoxy}$ during the measurement time under these experimental conditions (*10*). Since partial deprotonation of Tyr, that would give rise to a more intense Y8a band around 1600 cm^{-1}, may be involved at higher pH, the spectrum of

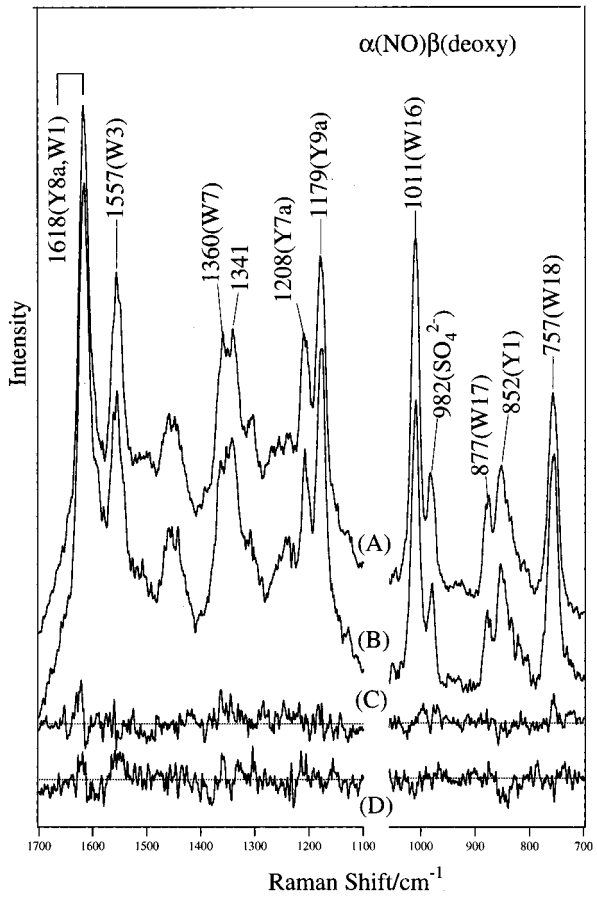

FIGURE 5: UVRR spectra of α(NO)*β*(deoxy) in the presence of IHP at pH 5.6 (A) and in the absence of IHP at pH 8.8 (B) and difference spectra with regard to deoxyHb: (C) deoxyHb at pH 6.7 − spectrum (A); (D) deoxy Hb at pH 8.8 − α(NO)*β*(deoxy) at pH 8.8 in the absence of IHP. The α(NO)*β*(deoxy) sample in the presence of IHP (5 mM) at pH 5.6 was equilibrated with 0.05 M acetate buffer. The spectrum of deoxyHb at pH 6.7 is the same as Figure 1(A). The deoxyHb and α(NO)*β*(deoxy) samples at pH 8.8 were equilibrated with 0.05 M Tris buffer. Each spectrum is an average of 8 spectra. The band marked by SO_4^{2-} means the totally symmetric stretching band of SO_4^{2-} ions.

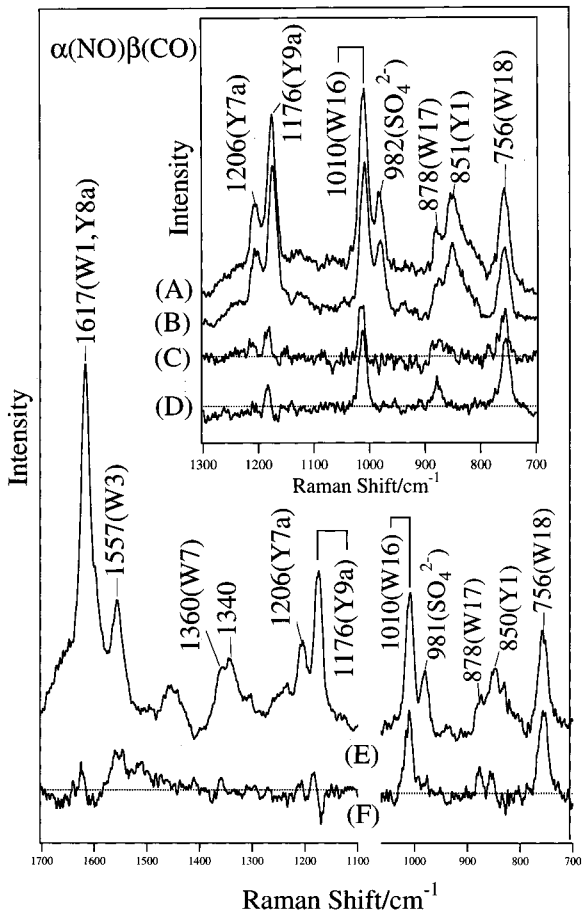

FIGURE 6: UVRR spectra of α(NO)*β*(CO) at pH 5.5 in the presence of IHP (A) and α(NO)*β*(CO) at pH 7.5 in the absence of IHP (B) and difference spectra: (C) deoxyHb at pH 6.7 − (A); (D) deoxyHb at pH 6.7 − (B); raw spectrum of α(NO)*β*(CO) at pH 8.8 in the absence of IHP (E), and its difference spectrum; (F) deoxy Hb (pH 6.7) − (E). The α(NO)*β*(CO) sample at pH 5.5 in the presence of IHP (5 mM) was equilibrated with 0.05 M acetate buffer. The α-(NO)*β*(CO) samples at pH 7.5 and pH 8.8 were equilibrated with 0.05 M phosphate and Tris buffer, respectively. The spectrum of deoxyHb at pH 6.7 is the same as Figure 1(A). Each spectrum is an average of 8 spectra. The band marked by SO_4^{2-} means the totally symmetric stretching band of SO_4^{2-} ions.

deoxyHb was measured at pH 8.8 (not shown), and used for the difference calculations described below. The difference spectra of $\alpha^{NO}\beta^{deoxy}$ [(A) and (B)] with regard to deoxyHb are depicted by traces (C) and (D), respectively. These difference spectra exhibit no clear peaks, indicating that the half-ligated $\alpha^{NO}\beta^{deoxy}$ at both pHs adopts the T structure, similar to deoxyHb irrespective of the presence or absence of IHP.

Figure 6 shows the UVRR spectrum of the mixed-ligated Hb, $\alpha^{NO}\beta^{CO}$, at pH 8.8 in the absence of IHP. Its spectra at pH 5.5 in the presence of IHP (A) and at pH 7.5 in the absence of IHP (B) are also shown in the inset together with their differences against deoxyHb at pH 6.7 [(C and (D)]. The difference spectrum, deoxyHb at pH 6.7 minus $\alpha^{NO}\beta^{CO}$ at pH 8.8 in the absence of IHP, is depicted by spectrum (F). We confirmed by EPR that no detectable ligand exchange occurred in the mixed-ligand Hb, $\alpha^{NO}\beta^{CO}$, under the present experimental conditions (*10*). Spectrum (F) is almost the same as Figure 1(C), meaning that the mixed-ligated $\alpha^{NO}\beta^{CO}$ in the absence of IHP at pH 8.8 adopts the R structure similar to COHb. However, this situation is changed when the pH is lowered. The intensities of the W16, W17, and W18 bands of Trp are stronger in spectra (A) than (B). The difference spectra for deoxyHb at pH 6.7 − $\alpha^{NO}\beta^{CO}$ at pH 5.5 and 7.5, represented by traces (C) and (D), respectively, exhibit similar patterns, but peak intensities are stronger in trace (D) than trace (C). Accordingly, Trp residues of $\alpha^{NO}\beta^{CO}$ in the presence of IHP at pH 5.5 stay in a more T-like structure.

Figure 7 plots the proportions of the five-coordinate α^{NO} heme in NOHb determined with EPR against pH. The proportions of the T-like contact evaluated by UVRR Trp bands under the assumption that deoxyHb and COHb at pH 6.7 adopt the 100% T and R structures, respectively, are also plotted against pH in the same figure. It is clear that the proportion of five-coordinate species decreases at higher pH and the transition pH from the five- to six-coordinate structure is higher in the presence of IHP. The proportion of the T-like contact deduced from UVRR at room temperature exhibits the same trend, although the percentage values are not in agreement with the amount of five-coordinate α hemes deduced from EPR at 77 K. The difference in the experimental temperature could be a possible origin of the

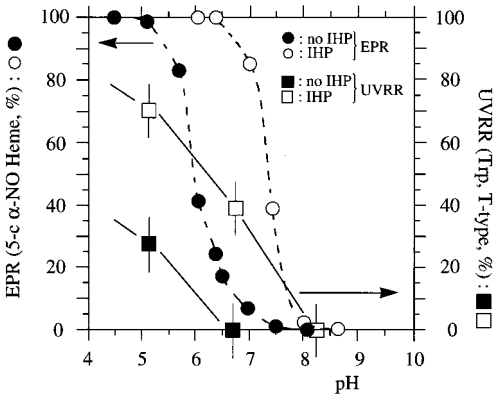

FIGURE 7: Proportion of the cleaved Fe−His bond of α heme in NOHb determined by EPR and proportion of the T-type contact of Trp residues at the subunit interface determined for NOHb by UVRR (see text). Squares and circles denote the UVRR and EPR data, respectively, and closed and open symbols represent the data for the solution in the absence and presence of IHP, respectively.

discrepancy, since the stabilities of hydrogen bonds and hence of quaternary structures are temperature dependent. Nevertheless, we emphasize that the behavior of the Trp residue at the α1−β2 interface is qualitatively correlated with the Fe−His bonding of α heme. The presence of such a qualitative correlation between the Fe−His bond and the α1−β2 interface contacts has been pointed out by recent RR studies (*27, 28*). It is clear that IHP shifts the pK_a of two equilibrium structures toward an alkaline side.

DISCUSSION

Correlation between the Fe−His Bond of the α Heme and the α1−β2 Subunit Interface Structure. NOHb has been extensively studied because it has been demonstrated from EPR (*12*−*14*), visible absorption (*11*), and RR (*15*) studies that the Fe−His bond of the α heme is cleaved in the presence of IHP. However, the structure of the α1−β2 subunit interface of NOHb has not been clarified so far. UVRR spectroscopy excited at 220−240 nm can sensitively monitor the structural changes of aromatic residues located in the α1−β2 subunit interface (*20, 21, 24*−*28*). Previous studies have demonstrated that the major intensity change of Trp UVRR bands upon the T−R transition arises from Trp-β37 (*22*) and that the frequency shift of Y8a and Y9a bands of Tyr upon the T−R transition is mainly due to α42- and α140-Tyr residues, while their intensity changes are due to α140- and β145-Tyr residues (*23, 38*). The results are consistent with the recent UVRR study on subunit-specific isotope labeling of recombinant HbA (*26*).

NOHb in the absence of IHP exhibited the UVRR spectrum of R structure at pH 6.7, but the spectrum changed upon the addition of IHP (Figure 2). The resultant subunit interface contains Tyr residues with R-like contact and Trp residues with R/T-intermediate contact. The proportion of the T-type contact of Trp exhibited qualitative correlation with the cleaved proportion of the Fe−His bond of the α heme (Figure 7). However, it should be stressed that the behaviors of Trp and Tyr bands are not always synchronous, meaning that the whole protein structures cannot be represented by simple two concept, that is, T and R structures, although individual residues may take two alternative structures. A recent UVRR study of Hb Kempsey (*27*) has also shown that Trp and Tyr signals do not develop in concert. In its time-resolved UVRR, Trp W3 difference develops much faster than the sigmoidal Y8a/Y8b bands of Tyr residues. Accordingly, we use T-like or R-like contact to describe the local structure of a given residue. The Tyr bands of NOHb behaved mostly R-like except for $\alpha^{NO}\beta^{deoxy}$.

The UVRR spectrum of the mixed-ligand $\alpha^{NO}\beta^{CO}$ in the presence of IHP indicated an intermediate state between the T and R structures as shown in the inset of Figure 6, similar to NOHb. This suggests that irrespective of the species of the sixth ligand bound to the β heme the subunit interface adopts an intermediate contact for Trp residues and R-like contact for Tyr residues, when NO is bound to the α heme in the presence of IHP. However, the content of the T structure evaluated with Trp bands does not always agree with the population of the α heme with the Fe−His bond cleaved.

In the case of half-NO-ligated Hb, $\alpha^{NO}\beta^{deoxy}$, both Tyr and Trp bands in UVRR spectra exhibited the characteristics of the T-structure similarly at pH 5.6 and 8.8. On the other hand, EPR showed that the population of the α^{NO} heme with the Fe−His bond broken is ∼100% at pH 5.5 but 50−60% at pH 8.8 in the presence of dithionite (not shown). Here again, the cleaved proportion of the Fe−His bond of α heme does not agree with the proportion of T-like contact at the α1−β2 interface evaluated from the Trp UVRR bands. The difference in temeprature of the two measurements might be a possible origin of the discrepancy. Nonetheless, there is a qualitative trend that the cleavage of the Fe−His bond of the α heme leads to the T-like α1−β2 interface structure, and the addition of IHP promotes both features. The effect of IHP is smaller at higher pH, and one reason is that the Fe−His bond is more stable at higher pH. The lack of complete correspondence between Fe−His bond cleavage and T-like subunit contacts is presumably due to the fact that ligand binding to the β heme appreciably affects the α1−β2 subunit contact, although it is mainly determined by the Fe−His bond of α heme. In fact, detailed comparison of UVRR spectra of NOHb and $\alpha^{NO}\beta^{deoxy}$ suggests that the Tyr contacts at the α1−β2 interface are more sensitive to ligand binding to β heme than the cleavage of the Fe−His bond of α heme.

Communication between the Heme Moiety and Subunit Interface. Figure 8 illustrates the main chain arrangements of deoxyHb at the α1−β2 contact region where significant rearrangements of residues occur upon the T → R transition (*39*). Three likely pathways of communication from the α heme to β heme have been proposed (*7*). In all of them, a change of the Fe−His bond of α heme is perceived first by Val-α93 (FG5). This residue communicates the change of the Fe−His bond to Tyr-α140 (HC2), which forms a hydrogen bond in T-like contact, and then it is communicated to Trp-β37. There is also another pathway that includes Val-α93 (FG5)→Arg-α92 (FG4)→Arg-β40 (C6)→Tyr-α42 (C7)→Asp-β99 (G1)→Val-β98 (FG5)→His-β92 (F8), in which Thr-α41 (C6) instead of Asp-β99 (G1) can also communicate the information to Val-β98 (FG5) through Tyr-β145 (HC2) (*7*). Other study suggests communication from the α heme to the β heme through a hydrogen bond between Asp-α94 and Trp-β37 which exists in the T-state but not in the R-state (*40*). In any cases, cleavage of the Fe−His bond in the α heme causes appreciable changes in the environ-

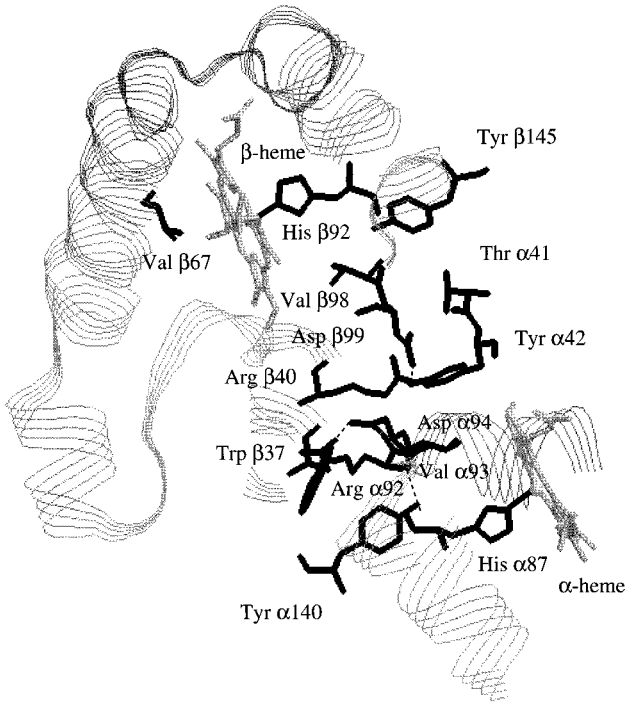

FIGURE 8: Main chain arrangement and orientation of amino acid side chains at α1−β2 contact of deoxyHbA. Tyr-α42, Tyr-α140, and Trp-β37 which are responsible for the present UVRR spectral changes are also contained. X-ray crystallographic coordinates are taken from the Protein Data Bank (*39*). The thick and thin broken lines denote the Fe−His bond and hydrogen bonds, respectively.

mental conditions of Tyr-α42, Tyr-α140, Tyr-β145, and Trp-β37. Accordingly, it is reasonable that UVRR spectral change of Trp-β37 has qualitative correlation with the cleavage of the Fe−His bond of the α heme. The recent X-ray crystallographic (*41*) as well as Raman studies (*28*) of β37 mutants together demonstrated a direct link between changes in the Fe−His bond and those of both Tyr-α140 and Trp-β37. These results are directly relevant to the present UVRR findings.

When NO binds to β hemes, it is thought that Val-β67 (E11) imposes steric hindrance to bound NO. However, the X-ray crystallographic analysis pointed out that movements of Val-β67 (E11) upon ligand binding to the β heme are not large but the change in the proximal side is rather large (*4, 5*). It means that the proximal His (His-β92) moves upon ligand binding and the neighboring Val-β98 (FG5) follows it in a way similar to that in the α subunit. Then, the information can proceed to the opposite direction through the communication pathway which was described above for the transmission of information from the α to the β subunit, and accordingly Tyr-β145 (HC2) and Tyr-α42 (C7) would be more sensitively influenced than Trp-β37. These two tyrosine residues would be sensitive when the β heme is six-coordinate but the α heme is five-coordinate. In fact, both $\alpha^{NO}\beta^{deoxy}$ (Figure 5A) and $\alpha^{NO}\beta^{NO}$ (Figure 3A) at pH 5.2−5.6 in the presence of IHP have the cleaved Fe−His bond of α heme, but the Tyr bands of the former and latter are T- and R-like, respectively. The Trp-β37 is less T-like in the latter than in the former.

However, we cannot rule out the idea that the role of the Fe−His bond of β heme is functionally different from that of the Fe−His bond of α heme, when the following facts are considered: $\alpha(Fe)_2\beta(porphyrin)_2$ Hb undergoes normal T−R transition upon ligation at the α subunits in the absence of the Fe−His bond of β heme. In this case, Tyr-α42 and Tyr-β145 must be influenced by the passageway originating from the α subunits. On the other hand, $\alpha(porphyrin)_2\beta(Fe)_2$ Hb is regarded as the T-(low affinity extreme) state at low pH regardless of the ligation at the β subunits because of the absence of the Fe−His bond of α heme (*42*). The UVRR spectrum of $\alpha(porphyrin)_2\beta(Fe)_2$ Hb, which has not yet been obtained, would be close to that of $\alpha^{NO}\beta^{deoxy}$ at pH 5.5 in the presence of IHP observed in this study. Presumably the ligand binding effects of β heme must be smaller in strength (of energetically smaller contribution) than those of α heme but disturb the qualitative correlation between Fe−His bond cleavage of α heme and the proportion of T-like α1−β2 contact estimated from UVRR.

The result of $\alpha^{NO}\beta^{deoxy}$ in the absence of IHP at pH 8.8 is to be noted. There is no migration of NO from the α to the β subunit during the experiment (*10*). The UVRR spectrum of $\alpha^{NO}\beta^{deoxy}$ suggests the T-like contact at the α1−β2 interface, but its EPR spectrum indicates that the six-coordinate state holds 50−60% in the α^{NO} heme (not shown). This may suggest that the coordination of an external ligand to the β heme also causes some movement of Trp-β37 and changes the α1−β2 contact toward the R-type. In fact, ligation of NO or CO to the β heme of $\alpha^{NO}\beta^{deoxy}$ in the absence of IHP changed the α1−β2 contact to yield the complete R structure, and the ligation in the presence of IHP caused the change from T- to half-R-like. This apparently inconsistent observation would also be interpreted by taking the ligand binding effects of the β heme mentioned above into consideration. Consequently, the factor that determines the interface contact is not only the Fe−His bond of the α heme but also the Fe−His bond of the β subunit which is caused by ligation to the β heme, although the strength of the effect of β heme is smaller than that of α heme.

The importance of the coordination of a ligand to the β heme is also noted for the half-ligated normal Hb, $\alpha^{O2}\beta^{deoxy}$, for which X-ray crystallographic analysis (*43, 44*) demonstrated a T-structure similar to deoxyHb, although its crystal was grown from poly(ethylene glycol). The fact that $\alpha^{O2}\beta^{deoxy}$ takes the T-structure means that the sum of free energy resulting from the structural changes of α hemes by ligand binding and from the subunit contacts at the α1−β2 interface is of a magnitude comparable to the lattice energy required to retain the structure of a whole molecule in the initially prepared crystal. A qualitatively similar conclusion is obtained with the α(Fe)β(Ni) metal hybrid Hb, $\alpha^{Fe}\beta^{Ni}$, for which the ^{1}H NMR study (*45*) demonstrated the presence of T-like contact at the α1−β2 interface even after CO was bound to the α heme in the presence of IHP at pH 7.4. In both $\alpha^{Fe-CO}\beta^{Ni}$ and $\alpha^{O2}\beta^{deoxy}$ Hbs, the Fe−His bond of α heme remains intact, but the quaternary structure takes the T structure.

Relation between the Fe−His Bond of α *Heme and Quaternary Structure.* UVRR results show that $\alpha^{NO}\beta^{CO}$ in the absence of IHP at pH 8.8 (Figure 6E) and in the presence of IHP at pH 5.5 (Figure 6A) takes R and half-R contact, respectively, with regard to Trp-β37. In contrast, Trp-β37 in $\alpha^{NO}\beta^{deoxy}$ was T-like under both conditions (Figure 5). This means that binding of CO to the β^{deoxy} heme causes a shift of the quaternary equilibrium to R but the structural change is more difficult for the latter than the former

conditions. One of the differences between $\alpha^{NO}\beta^{deoxy}$ in the presence of IHP at pH 5.5 and in its absence at pH 8.8 is population of the cleaved Fe−His bond of the α heme. On the basis of the EPR spectra observed (not shown), the Fe−His bond is retained by 50−60% of the α hemes in the absence of IHP at pH 8.8 but by no α hemes in the presence IHP at pH 5.5 (not shown). This suggests that cleavage of the Fe−His bond of α heme stabilizes the T-type contacts at the α1−β2 interface. Liddington et al. (*44*) pointed out from the structural analysis of $\alpha^{O2}\beta^{deoxy}$ Hb that the preservation of the six-coordinate planar structure of the α heme within the T structure increases the conformational strain and thus results in unstability of the T structure. For an abnormal Hb, Hb Yakima (Asp-β99 → His), known as a high-affinity Hb (*46*), the high affinity has been attributed to the lack of a hydrogen bond between Tyr-α42 and Asp-β99 (Figure 8) in the α1−β2 interface which normally stabilizes the T structure. Accordingly, the higher oxygen affinity to the β heme of $\alpha^{NO}\beta^{deoxy}$ in the absence of IHP at pH 8.8 than that to ordinary deoxyHb is also consistent with the unstability of the T structure at the α1−β2 interface. In this sense, the Fe−His bond of α hemes seems to influence the quaternary structural transition and oxygen affinity.

In conclusion, the Fe−His bond of α hemes is not the sole origin of the structural changes at the α1−β2 interface, because $\alpha^{NO}\beta^{deoxy}$ exhibits T-like UVRR spectra regardless of pH and IHP while the proportion of the cleaved Fe−His bond of α hemes is varied. There are, however, appreciable differences in the stability of the T-like contact of the α1−β2 interface between the absence and presence of the Fe−His bond of the α heme. Ligand binding to β hemes also changes the α1−β2 interface contact through the movement of the proximal His (β92, F8) and thus the quaternary structure.

REFERENCES

1. Monod, J., Wyman, J., and Changeux, J. P. (1965) *J. Mol. Biol. 12*, 88−118.
2. Perutz, M. F. (1970) *Nature 228*, 726−739.
3. Perutz, M. F. (1979) *Annu. Rev. Biochem. 48*, 327−386.
4. Perutz, M. F., Fermi, G., Luisi, B., Shaanan, B., and Liddington, R. C. (1987) *Acc. Chem. Res. 20*, 309−321.
5. Baldwin, J., and Chothia, C. (1979) *J. Mol. Biol. 129*, 175−220.
6. Fung, L. W.-M., and Ho, C. (1975) *Biochemistry* 14, 2526−2535.
7. Ho, C. (1992) *Adv. Protein Chem. 43*, 152−312.
8. Gibson, Q. H., and Roughton, F. J. W. (1957) *Proc. R. Soc. London B 147*, 44−56.
9. Huang, T.-H. (1979) *J. Biol. Chem. 254*, 11467−11474.
10. Yonetani, T., Tsuneshige, A., Zhou, Y., and Chen, X. (1998) *J. Biol. Chem. 273*, 20323−20333.
11. Perutz, M. F., Kilmartin, J. V., Nagai, K., Szabo, A., and Simon, S. R. (1976) *Biochemistry 15*, 378−387.
12. Salhany, J. M., Ogawa, S., and Shulman, R. G. (1975) *Biochemistry 14*, 2180−2190.
13. Nagai, K., Hori, H., Yoshida, S., Sakamoto, H., and Morimoto, H. (1978) *Biochim. Biophys. Acta 532*, 17−28.
14. Hille, R., Olson, J. S., and Palmer, G. (1979) *J. Biol. Chem. 254*, 12110−12120.
15. Nagai, K., Welborn, C., Dolphin D., and Kitagawa, T. (1980b) *Biochemistry 19*, 4755−4761.
16. Nagai, K., Kitagawa, T., and Morimoto, H. (1980a) *J. Mol. Biol. 136*, 271−289.
17. Nagai, K., and Kitagawa, T. (1980) *Proc. Natl. Acad. Sci. U.S.A. 77*, 2033−2037.
18. Harada, I., Miura, T., and Takeuchi, H. (1986) *Spectrochim. Acta 42A*, 307−312.
19. Kitagawa, T. (1992) *Prog. Biophys. Mol. Biol. 58*, 1−18.
20. Rodgers, K. R., Su, C., Subramaniam, S., and Spiro, T. G. (1992) *J. Am. Chem. Soc. 114*, 3697−3709.
21. Rodgers, K. R., and Spiro, T. G. (1994) *Science 265*, 1697−1699.
22. Nagai, M., Kaminaka, S., Ohba, Y., Nagai, Y., Mizutani, Y., and Kitagawa, T. (1995) *J. Biol. Chem. 270*, 1636−1642.
23. Nagai, M., Imai, K., Kaminaka, S., Mizutani, Y., and Kitagawa, T. (1996) *J. Mol. Struct. 379*, 65−75.
24. Huang, S., Peterson, E. S., Ho, C., and Friedman, J. M. (1997) *Biochemistry 36*, 6197−6206.
25. Huang, J., Juszczak, L. J., Peterson, E. S., Shannon, C. F., Yang, M., Huang, S., Vidugiris, G. V. A., and Friedman, J. M. (1999) *Biochemistry 38*, 4514−4525.
26. Hu, X., and Spiro, T. G. (1997) *Biochemistry 36*, 15701−15712.
27. Hu, X., Rodgers, K. R., Mukerji, I., and Spiro, T. G. (1999) *Biochemistry 38*, 3462−3467.
28. Peterson, E. S., and Friedman, J. M. (1998) *Biochemistry 37*, 4346−4357.
29. Nagai, M., Nishibu, M., Sugita, Y., Yoneyama, Y., Jones, R. T., and Gordon, S. (1975) *J. Biol. Chem. 250*, 3169−3173.
30. Kaminaka, S., and Kitagawa, T. (1995) *Appl. Spectrosc. 49*, 685−687.
31. Song, S., and Asher, S. A. (1991) *Biochemistry 30*, 1199−1205.
32. Kaminaka, S., and Kitagawa, T. (1992a) *Appl. Spectrosc. 46*, 1804−1808.
33. Dudik, J. M., Johnson, C. R., and Asher, S. A. (1985) *J. Chem. Phys. 82*, 1732−1740.
34. Miura, T., Takeuchi, H., and Harada, I. (1988) *Biochemistry 27*, 88−94.
35. Miura, T., Takeuchi, H., and Harada, I. (1989) *J. Raman Spectrosc. 20*, 667−671.
36. Harada, I., and Takeuchi, H. (1986) *Adv. Spectrosc. 13*, 113−175.
37. Kaminaka, S., and Kitagawa, T. (1992b) *J. Am. Chem. Soc. 114*, 3256−3260.
38. Nagai, M., Wajcman, H., Lahary, A., Nakatsukasa, T., Nagatomo, S., and Kitagawa, T. (1999) *Biochemistry 38*, 1243−1251.
39. Fermi, G., Perutz, M. F., Shaanan, B., and Fourme, R. (1984) *J. Mol. Biol. 175*, 159−174.
40. Ishimori, K., Imai, K., Miyazaki, G., Kitagawa, T., Wada, Y., Morimoto, H., and Morishima, I. (1992) *Biochemistry 31*, 3256−3264.
41. Kavanaugh, J. S., Weydert, J. A., Rogers, P. H., and Arnone, A. (1998) *Biochemistry 37*, 4358−4373.
42. Fujii, M., Hori, H., Miyazaki, G., Morimoto, H., and Yonetani, T. (1993) *J. Biol. Chem. 268*, 15386−15393.
43. Brzozowski, A., Derewenda, Z., Dodson, E., Dodson, G., Grabowski, M., Liddington, R., Skarzynski, T., and Vallely, D. (1984) *Nature (London) 307*, 74−76.
44. Liddington, R., Derewenda, Z., Dodson, G., and Harris, D. (1988) *Nature (London) 331*, 725−728.
45. Shibayama, N., Inubushi, T., Morimoto, H., and Yonetani, T. (1987) *Biochemistry 26*, 2194−2201.
46. Novy, M. J., Edwards, M. J., and Metcalfe, J. (1967) *J. Clin. Invest. 46*, 1848−1854.

BI990567W